

Optimum Wavelet Based Homomorphic Medical Image Fusion Using Hybrid Genetic – Grey Wolf Optimization Algorithm

Ebenezer Daniel

Abstract— Medical image fusion techniques have been widely used in various clinical applications. Generalized homomorphic filters have Fourier domain features of input image. In multi modal medical image fusion discrete wavelet transform based techniques provides more features and is performed over Fourier spectrum. In this paper, we proposed a Homomorphic wavelet fusion which is called Optimum Homomorphic Wavelet Fusion (OHWF) using Hybrid Genetic – Grey Wolf Optimization (HG-GWO) Algorithm. In OHWF, which consist of logarithmic and wavelet domain information of input images. The wavelet based homomorphic fusion consists of multi level decomposition features of input image. In our proposal, the approximation coefficients of modality1 (anatomical structure) and optimum scaled detailed coefficients of modality2 are given to adder1. In adder 2, the optimum scaled detailed coefficients of modality 1 and approximation coefficients of modality 2 are added together. The resultants of adder 1 and adder 2 are fused together using pixel based averaging rule. Firstly, the proposed fusion approach is validated for MR-SPECT, MR-PET, MR-CT and MR T1-T2 image fusion using various fusion evaluation indexes. Later, the conventional grey wolf optimization is modified with genetic operator. Experimental results show that, the proposed approach outperforms state-of-the-art fusion algorithms in terms of both structural and the functional information in the fused image.

Index Terms—Homomorphic Filtering, Wavelet Transform Image fusion, Medical imaging, Grey Wolf Optimization Algorithm, Genetic Algorithm

I. INTRODUCTION

Medical image fusion techniques provide better biomedical information for clinical evaluation. In medical diagnosis multimodal fused images has more significant role than individual image. The multi model medical image fusion is the process of combining compliment fusion techniques for clinical analysis. Recent literatures in medical image fusion say that multi scale image fusion has more significant role in data fusion. The multi scale based decomposition is mainly performed using transformation functions. V. Bhateja et al., proposed a hybrid wavelet and Contourlet transform based medical image fusion approach, in which, multi level fusion is performed for MR-CT fusion [1]. In medical image fusion,

efficient functional mapping as well as structural mapping is required. The Curvelet domain coefficients have more structural features, R. Srivastava et al., proposed a Curvelet based medical image fusion technique [2]. G. Bhatnagar et al., proposed a Non Subsampled Contourlet Transform (NSCT) in medical image fusion, in which high frequency and low frequency of complementary modalities are fused based on individual fusion rules [3]. Recently introduced fusion technique called Moving Frame based Decomposition Framework (MFDF) is introduced to encode local geometry of an image [4]. Liu et al introduced a Non Subsampled Shearlet Transform (NSST) based approach for image fusion, in which they transferred more edges and texture information of source image into fused image [5]. Recently hybrid Fuzzy Contourlet based technique was used for multimodal medical image fusion, in which Contourlet domain high frequency and approximation features were fused using fuzzy based technique [6]. Recently Laplacian filter based decomposition techniques used in multilevel feature decomposition [7]. Y. Yang et al., proposed a Fuzzy logic based non Subsampled Contourlet domain medical image fusion technique, in which they were tested MR-CT, MR-SPECT and MR-PET multimodal medical images [8]. L. Wang et al proposed Gaussian density based Shift Invariant Shearlet Transform (SIST) based multimodal fusion approach [9]. Wavelet transform based techniques have efficient role in multilevel decomposition [10] in multimodal image fusion. In past, various advancements were developed in the field of wavelet based decomposition. P. Chai et al., proposed a Quaternion Wavelet Transform (QWT) based multilevel decomposition technique, in which they implemented QWT technique in medical images, multi-focus images, infrared-visible images, and remote sensing images [11]. The Discrete Fractional Wavelet Transform (DRWT) based technique can provide multi level time fractional frequency domain features of the image [12]. Z. Zhu et al., introduced a dictionary learning based technique for multimodal medical image fusion was performed based on sparse representation and coefficient fusion [13]. C. I Chen proposed Log Gabor Wavelet based approach for medical image fusion, in which Log filter based structure mapping and Intensity Hue Saturation (IHS) transform based functional mapping were performed [14]. J. Du et al., introduced saliency feature based technique, in which they preserved high resolution edge information of the image [15]. S. C Chavan et al., proposed a Non Subsampled Rotated Complex Wavelet transform (NSRCxWT) based medical image fusion, in which they used both averaging and

Ebenezer Daniel is with Department of Electronics & Communication Engineering, Vignan's Foundation for Science, Technology & Research, Andhra Pradesh, India 522213. (Email: ebydaniel89@gmail.com).

maximizing fusion rule for complementary fusion [16]. In last decade, various soft computing techniques were applied in multimodal image fusion applications. Kavitha and Chellamuthu were proposed Ant Colony Optimization (ACO) based edge feature detection and fused using Pulse Coupled Neural Network. (PCNN) [17]. There were various soft computing techniques implemented in image fusion applications such as, Quantum-Behaved Particle Swarm Optimization (QPSO) [18], deep Convolutional neural network [19], human visual system (HVS) [20], Neuro Fuzzy [21] and Grey Wolf Optimization (GWO) [22,23] techniques. Intelligent medical image fusion techniques are used in computer aided brain surgery, Alzheimer's treatment, tumor detection and other clinical diagnosis [24-30]

In this paper, we proposed an optimum wavelet domain homomorphic filter which provides multi level decomposition in homomorphic domain. The optimum scale values are selected using a novel optimization approach called Hybrid Genetic Grey Wolf Optimization algorithm.

The organization of this paper is as follows. Section 2 describes the generalized homomorphic filtering and the need of multi scale filtering. Section 3 presents the proposed wavelet based homomorphic fusion in detail. Section 4 discusses the results and discussion. Lastly, Section 6 presents the conclusions.

II. GENERALIZED HOMOMORPHIC FILTERING

Homomorphic filtering is an image enhancement technique, which decomposes the original image. The input image $f_{(x,y)}$ is the product of illumination $i_{(x,y)}$ and reflection $r_{(x,y)}$ coefficients as shown in Eq (1).

$$f_{(x,y)} = i_{(x,y)} r_{(x,y)} \quad (1)$$

The original image is operated using logarithmic filter. The resultant $z_{(x,y)}$ is the sum of illumination and reflection coefficients in logarithmic domain as shown in Eq (2).

$$z_{(x,y)} = \ln(i_{(x,y)}) + \ln(r_{(x,y)}) \quad (2)$$

The decomposed components of logarithmic coefficients are transformed using Discrete Fourier Transform (DFT) as shown in Eq (3). The resultant of DFT is operated using a selective filter $H_{(u,v)}$ as shown in Eq (4). Where $S_{(u,v)}$ is the selective filtered image.

$$z_{(u,v)} = F_{i(u,v)} + F_{r(u,v)} \quad (3)$$

$$S_{(u,v)} = H_{(u,v)} F_{i(u,v)} + H_{(u,v)} F_{r(u,v)} \quad (4)$$

$$S_{(u,v)} = H_{(u,v)} Z_{(u,v)} \quad (5)$$

The resultant homomorphic image is in logarithmic frequency domain. For getting the spatial domain information, the Inverse Fourier transform of the image is obtained using Eq (5). The resultant image consist of both illumination and reflection coefficients in logarithmic range as given in Eq (6).

$$S_{(x,y)} = F^{-1} S_{(u,v)} \quad (6)$$

$$S_{(x,y)} = F^{-1} \{H_{(u,v)} F_{i(u,v)}^{-1}\} + F^{-1} \{H_{(u,v)} F_{r(u,v)}^{-1}\} \quad (7)$$

$$S_{(x,y)} = i'_{(x,y)} + r'_{(x,y)} \quad (8)$$

In second stage of homomorphic filtering the exponential of the image is calculated using Eq (7). The output image consist both illumination as well as reflection coefficients in time domain as shown in Eq (8).

$$\begin{aligned} g_{(x,y)} &= e^{S_{(x,y)}} \\ &= e^{i'_{(x,y)} + r'_{(x,y)}} \\ &= e^{i'_{(x,y)}} e^{r'_{(x,y)}} \\ &= i_{0(x,y)} r_{0(x,y)} \end{aligned} \quad (9)$$

The final homomorphic output image is given in the Eq (9). It consists of illumination coefficients which represent low frequency components and reflection coefficients represent the high frequency components. The conventional flow of homomorphic filtering is given in Fig. 1.

A. Need of multi scale decomposition in homographic filter

The conventional homomorphic filtering consists of two levels scaling such as illumination coefficients and reflection coefficients. In medical imaging applications multi scaling is an essential way for extracting the soft and hard tissue details. In our proposed approach, discrete wavelet transform is introduced for multilevel decomposition in homomorphic filtering. Wavelet transform can divide the input signal into multi-level bands, which provides enhanced details of soft tissues as well as hard tissues in medical imaging.

B. Proposed wavelet based homographic filter

Our proposed technique is an optimum multi scale homomorphic filter, in which multi scale decomposition is performed using wavelet transform as shown in Fig. 2. Original image consist of illumination as well as reflection coefficients as given in Eq (1), which is transformed to logarithmic operators and the resultant image as given in Eq (2), and the output of logarithmic filter is transformed in to wavelet domain.

$$W_{1\varphi(j_0, m, n)} = \frac{1}{\sqrt{MN}} \sum_{x=0}^{M-1} \sum_{y=0}^{N-1} Z_{(x,y)} \varphi_{(j_0, x, y)} \quad (10)$$

$$W_{1\psi(j, m, n)} = \frac{1}{\sqrt{MN}} \sum_{x=0}^{M-1} \sum_{y=0}^{N-1} Z_{(x,y)} \psi^i_{(j_0, x, y)}$$

$$W_{2\varphi(j_0, m, n)} = \frac{1}{\sqrt{MN}} \sum_{x=0}^{M-1} \sum_{y=0}^{N-1} Z_{(x,y)} \varphi_{(j_0, x, y)} \quad (11)$$

$$W_{2\psi(j, m, n)} = \frac{1}{\sqrt{MN}} \sum_{x=0}^{M-1} \sum_{y=0}^{N-1} Z_{(x,y)} \psi^i_{(j_0, x, y)}$$

The decomposed low pass and high pass filtered features of modality 1 and modality 2 are given in Eq (10) and Eq (11) respectively, where $i = \{H, V, D\}$, which provides horizontal, vertical and diagonal details of the input modality.

$$Z_{1(u,v)} = W_{2\varphi(j_0, m, n)} + W_{1\psi(j, m, n)} \quad (12)$$

$$Z_{2(u,v)} = \sigma_1 W_{\varphi}(j_0, m, n) + \sigma_2 W_{\psi}(j, m, n) \quad (13)$$

In which, $Z_{1(u,v)}$ and $Z_{2(u,v)}$ are the adder 1 and adder 2 outputs respectively.

$$Z_{fused} = Average(Z_{1(u,v)}, Z_{2(u,v)}) \quad (14)$$

$$Z_{(x,y)} = W^{-1}(Z_{(u,v)}) \quad (15)$$

$$g_{(x,y)} = e^{Z_{(x,y)}} \quad (16)$$

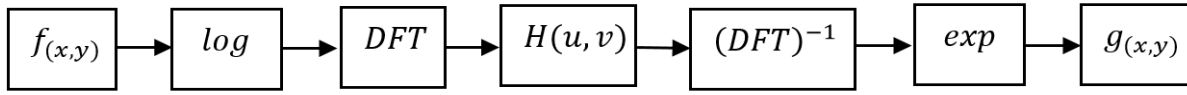


Fig. 1 Block diagram of generalized homomorphic filtering technique

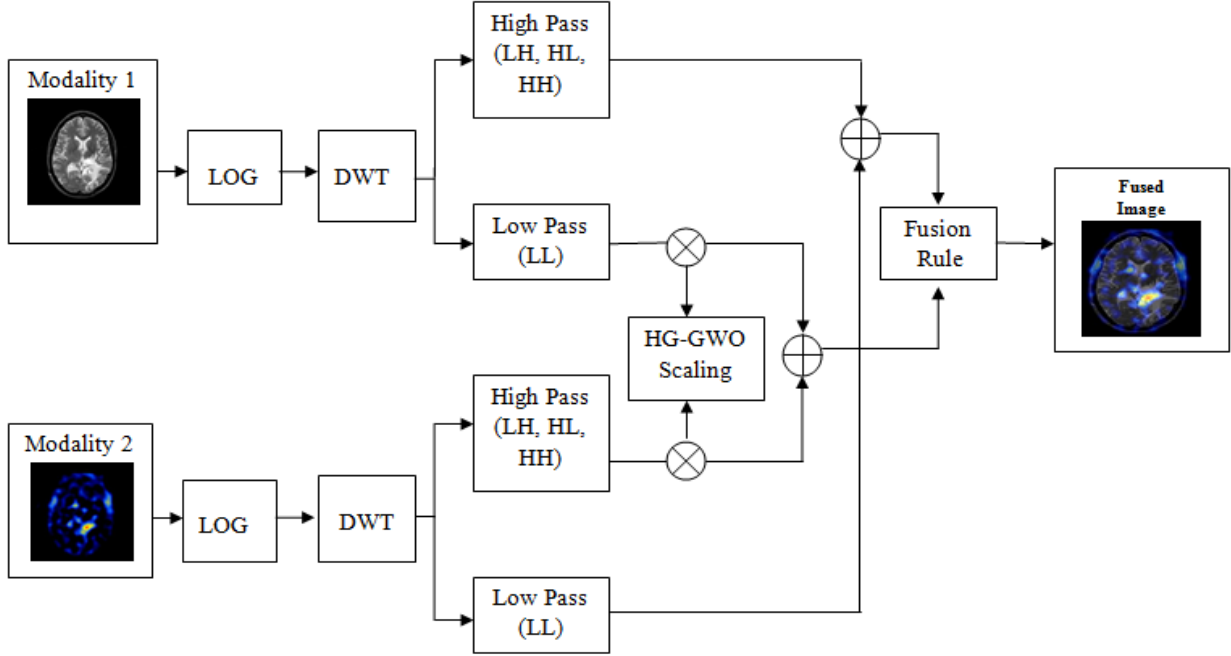


Fig. 2 Block diagram of proposed wavelet based homographic fusion technique

In which, $Z_{(u,v)}$ is the fused wavelet homomorphic output, as given in Eq (14). The $g_{(x,y)}$ is the spatial domain fused image as given in Eq (16).

III. HYBRID GENETIC BASED GREY WOLF OPTIMIZATION

This section is divided into following 3 sub sections,

- Grey wolf optimization
- Need of hybrid grey wolf optimization
- Proposed hybrid genetic grey wolf optimization

A. Grey Wolf Optimization

Grey Wolf Optimization is the one of the biologically inspired optimization algorithm used in various fusion applications in literature[22, 23]. The GWO algorithm imitates the hunting nature of grey wolf family, they usually prefer to be in a pack. They have a strict social dominant 4 level hierarchy, size of grey wolves pack is varying from 5 to 12 in number. In grey wolf social hierarchy, the best grey wolf candidate called alpha (α), they are the dominant wolves in the pack. The second best in hierarchy called beta (β), they are the subordinates to the alpha wolves. If the alpha wolves are absence in the pack then beta wolves will lead the pack. The lowest ranking wolves are called omega (ω). The omega wolves need to submit to all other wolves and they are allowed to eat last in a pack. The wolves other than alpha, beta or omega in their pack are called delta (δ). The delta wolves need to obey alpha and beta level wolves but dominate over omega wolves in their pack [31].

The mathematical modeling of GWO algorithm consists of three stages, tracking, encircling and attacking prey [31]. The mathematical model for encircling the prey can be represents in the following equations:

$$\vec{D} = |\vec{C} \cdot \vec{X}_{p(t)} - \vec{X}(t)| \quad (15)$$

$$\vec{X}(t+1) = \vec{X}_{p(t)} - \vec{A} \cdot \vec{D} \quad (16)$$

Where t represents the current iteration, \vec{A} and \vec{C} represents the coefficient vectors, $\vec{X}_{p(t)}$ is the position vector of prey, \vec{X} is the position vector of the grey wolf, \vec{A} and \vec{C} are calculated using Eq 15 and Eq16.

$$\vec{A} = 2\vec{a} \cdot \vec{r}_1 - \vec{a} \quad (17)$$

$$\vec{C} = 2 \cdot \vec{r}_2 \quad (18)$$

In which, \vec{a} is a variable, linearly decreasing from 2 to 0 over the course of iteration. Here, \vec{r}_1 and \vec{r}_2 are the random vectors, as given in Eq 17 and Eq16. The grey wolves can update their position anywhere in search space based on the random variables \vec{r}_1 and \vec{r}_2 [31, 32].

The hunt is usually lead based on the social hierarchy given in Fig.3. The hunting nature can be mathematically expressed using the following equations:

$$\left. \begin{aligned} \vec{D}_\alpha &= |\vec{C}_1 \cdot \vec{X}_\alpha - \vec{X}| \\ \vec{D}_\beta &= |\vec{C}_2 \cdot \vec{X}_\beta - \vec{X}| \\ \vec{D}_\delta &= |\vec{C}_3 \cdot \vec{X}_\delta - \vec{X}| \end{aligned} \right\} \quad (19)$$

$$\left. \begin{aligned} \vec{X}_1 &= \vec{X}_\alpha - \vec{A}_1 \cdot (\vec{D}_\alpha) \\ \vec{X}_2 &= \vec{X}_\beta - \vec{A}_2 \cdot (\vec{D}_\beta) \\ \vec{X}_3 &= \vec{X}_\delta - \vec{A}_3 \cdot (\vec{D}_\delta) \end{aligned} \right\} \quad (20)$$

$$\vec{X}(t+1) = \frac{\vec{X}_1 + \vec{X}_2 + \vec{X}_3}{3} \quad (21)$$

In which, the first three solutions are considered as optimum and remaining solutions are discarded, in which \vec{X} provides the average of best three solutions. Grey wolves finish the hunt by attacking the prey when it stops moving. If $|A| < 1$ then grey wolves attack towards the prey and if $|A| > 1$ then they diverge from the current prey and find a fitter one.

B. Need of Hybrid Grey Wolf Optimization

The variable \vec{a} is linearly selected whereas variables \vec{r}_1 and \vec{r}_2 are randomly fixing. The drawback of GWO is that, randomly selected variables which deciding the optimum position. In this paper, we introduced a hybrid genetic algorithm based grey wolf optimization for overcoming the limitations of conventional GWO. In which, GWO technique performs the optimum prey position meanwhile genetic algorithm selects the optimum control variables \vec{r}_1 and \vec{r}_2 .

C. Proposed Hybrid Genetic based Grey Wolf Optimization

The prime motivation of hybrid HG-GWO algorithm is to combine the advantages of genetic algorithm in conventional grey wolf algorithms for overcoming the static scales selection problem in GWO. The conventional grey wolf optimization consists of randomly selected control elements \vec{r}_1 and \vec{r}_2 , the static scale values might leads to the local minima region. In proposed technique, genetic operators such as: cross over and mutations are included to select the optimum control parameters. The implementation parameters are given in Table. 1. The details of HG-GWO are presented in following three subsections.

1) Generation of initial population

The GWO and GA are population based optimization algorithms. In HG-GWO, which generates population consist of n_1 number of positions for grey wolfs and n_2 number of initial population for GA. In HG-GWO, range of n_1 can be 20, 50,100,200 or any higher values, whereas the range of n_2 is 10, 20, 50 or any least values and n_2 should be lesser than n_1 in each iteration.

2) Optimum Selection of control parameters

During the hunting process of grey wolfs, firstly they encircle the prey and make sure that the prey is not moving. The mathematical modeling of encircling is given in Eq 14-20. In HG-GWO, two control parameters namely \vec{r}_1 and \vec{r}_2 is selected using genetic operators. The conventional GA having static crossover value and mutation as reported in various literatures. In HG-GWO, dynamic crossover ratio and mutation ratio is used ,which consist of following 3 steps : 1) ranking all the population based on the fitness 2) find the average value of fitness value and fixed as threshold value 3) discarding all the population with least fitness than threshold value with new population [31,32].

3) Generating the social hierarchy

In Grey wolf family, the hunting is leaded according to their social hierarchy. The selection of the optimum position is based on the fitness, where, X_α =the first search agent, X_β =the second search agent and, X_γ =the third search

agent. The direction and position of pack is calculated based on the Eq 14-20. The flow chart for hybrid HG-GWO is given in Fig 2.

IV. RESULTS AND DISCUSSION

In this section, we have analyzed the performance of the proposed fusion technique OWHF technique. The proposed OWHF is tested on various MR-SPECT, MR-PET, MR-CT and MR-T1-T2 input modalities. The database images used for our fusion analysis are available in <http://www.med.harvard.edu/AANLIB/home.html>.

The implementation results of proposed HG-GWO are given in Table 1. The optimum scale values obtained using proposed HG-GWO are listed in Table 2. In optimum weight analysis, σ_1 best and σ_2 best are the optimum values corresponding to input modality 1 and modality 2. All the computational experiments in this work were performed using Matlab 2010a on a PC with Pentium dual core processor and speed 2.30.

TABLE 1
Implementation results of HG-GWO

n_1 number of positions for grey wolfs	50
n_2 number of initial population for GA	20
Cross over ratio	Dynamic
Mutation ratio	Dynamic
Number of GWO iterations	50
Number of GA iterations	30

TABLE 2
Results of optimum scale values using HG-GWO

Type of image	σ_1	σ_2
MR-SPECT	0.2412	0.0141
MR-PET	0.4675	0.0352
MR-CT	0.5105	0.2302
MR-T1-T2	0.4813	0.3264

A. Quantitative and qualitative analysis of OWHF fusion technique

In this section, the proposed fusion technique is tested for MR-SPECT, MR-PET, MR-CT and MR-T1-T2 modalities. The quantitative results of the proposed OWHF based fusion technique is evaluated based on various matrices such as edge quality ($Q^{AB/F}$) [33], Mutual Information (MI) [9, 34], Entropy (E) [33], and Standard Deviation (STD) [35]. The proposed fusion technique is compared with the various existing fusion algorithms such as DCT [36], DWT [37], FFT [38] and IHS [39] and also compared with well-known optimization algorithms such as GA and PSO. The examples of 2 cases of input medical image models are given in Fig.5 and Fig. 6.

B. MR-SPECT Medical image Fusion

In this section, MR and SPECT images are fused using the proposed OWHF technique. Examples of fused MR-SPECT dataset images are given in Fig.8, in which metabolic information of SPECT is mapped over the anatomical feature of MR image. The quantitative results of MR-SPECT fusion for dataset1 and dataset 2 are given in Tables3 and 4. With regard to the attained results in Tables 1 and 2, the proposed technique can reveal superior results in terms of mutual information, signal quantity and edge information compared to the existing techniques.

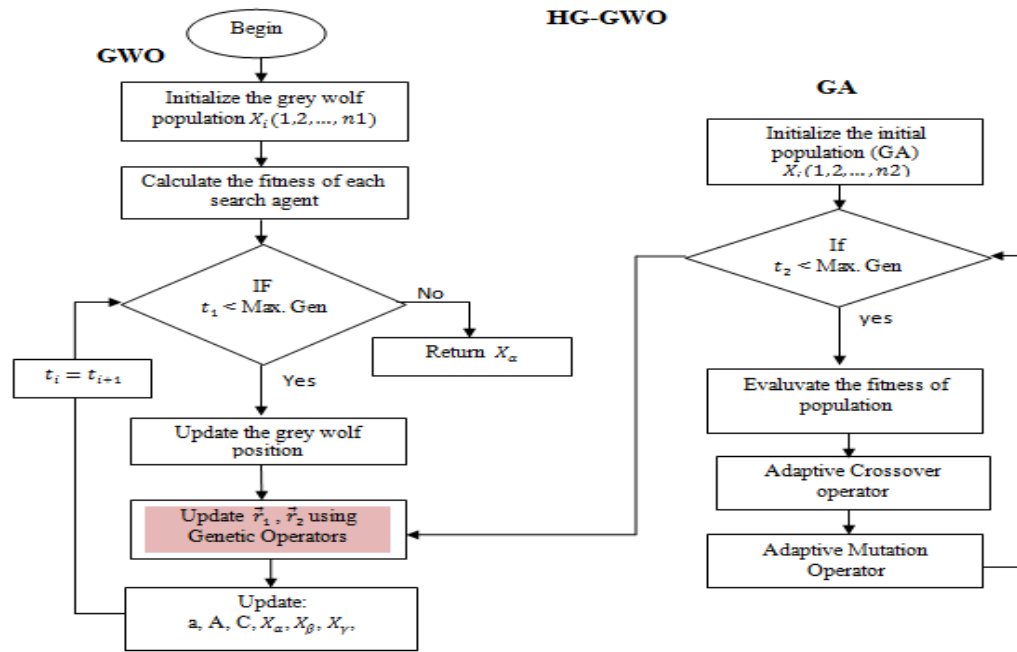


Fig.3 Flow chart of hybrid genetic grey wolf optimization algorithm

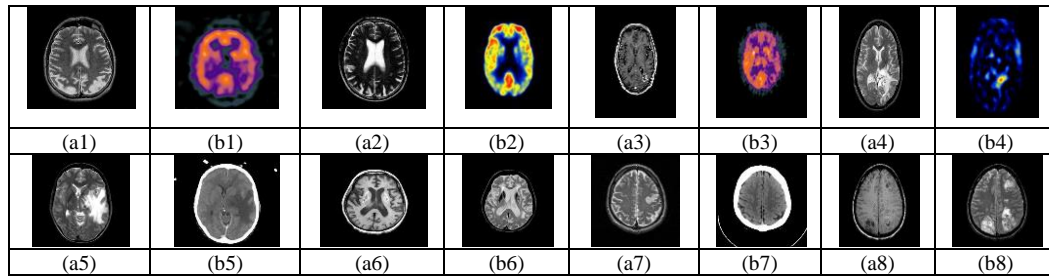


Fig.4. Input data sets : (a1),(b1) and (a2),(b2) are MR- SPECT input images, (a3),(b3) and (a4),(b4) are MR- PET input images, (a5),(b5) and (a7),(b7) are MR- CT input images, (a6),(b6) and (a8),(b8) are MR- T1-T2 input images

TABLE 3
RESULTS OF CASE1 MR-SPECT-IMAGE FUSION ANALYSIS

	DCT [10]	DWT [13]	FFT [11]	IHS [38]	OHWF-GA	Proposed
MI	2.3586	3.1351	3.2415	3.5214	3.8412	3.9426
Entropy	3.1201	4.7516	4.9534	5.1142	5.7564	5.9560
$Q^{AB/F}$	0.1285	0.1314	0.1502	0.1267	0.2056	0.2256
STD	48.4182	56.6352	61.2376	59.2354	73.5624	78.0651

TABLE 4
RESULTS OF CASE 2 MR-SPECT-IMAGES FUSION ANALYSIS

	DCT [10]	DWT [13]	FFT [11]	IHS [38]	OHWF-GA	Proposed
MI	2.7965	3.2341	3.6210	3.8514	4.4214	4.7283
Entropy	4.1256	5.4213	5.3541	5.6327	5.8854	5.9861
$Q^{AB/F}$	0.0854	0.0527	0.1031	0.0887	0.1726	0.1924
STD	57.5641	61.2350	58.3641	59.6351	68.2750	71.8351

TABLE 5
RESULTS OF CASE1 MR-PET-IMAGE FUSION ANALYSIS

	DCT [10]	DWT [13]	FFT [11]	IHS [38]	OHWF-GA	Proposed
MI	2.8745	3.0214	2.9685	3.2415	3.5471	3.8094
Entropy	4.5451	4.9204	4.7521	5.1124	5.5023	5.8135
$Q^{AB/F}$	0.0481	0.0621	0.0741	0.0687	0.1240	0.1526
STD	41.2543	44.5219	50.2341	47.3625	61.3623	68.4725

TABLE 6
RESULTS OF CASE2 MR-PET-IMAGE FUSION ANALYSIS

	DCT [10]	DWT [13]	FFT [11]	IHS [38]	OHWF-GA	Proposed
MI	2.4517	2.6324	3.1024	2.8451	3.4210	3.8371
Entropy	3.3126	3.5124	3.9874	3.6851	4.1254	4.8120
$Q^{AB/F}$	0.0841	0.0712	0.1042	0.1204	1.4102	1.6530
STD	2.4517	2.6324	3.1024	2.8451	3.5210	3.7453

TABLE 7
RESULTS OF CASE1 MR-CT-IMAGE FUSION ANALYSIS

	DCT [10]	DWT [13]	FFT [11]	IHS [38]	OHWF-GA	Proposed
MI	2.8412	3.1475	3.2134	3.5721	3.7241	3.9706
Entropy	3.6541	3.9412	4.0231	4.3541	4.8121	5.0143
$Q^{AB/F}$	0.0415	0.0652	0.0748	0.0875	0.1241	0.1586
STD	45.5210	53.2651	61.2351	64.4571	72.2327	78.9420

TABLE 8
RESULTS OF CASE2 MR-CT-IMAGE FUSION ANALYSIS

	DCT [10]	DWT [13]	FFT [11]	IHS [38]	OHWF-GA	Proposed
MI	2.8741	3.2014	2.9124	3.4102	3.9812	4.0723
Entropy	3.6545	4.1207	3.8231	4.3145	4.7125	5.3854
$Q^{AB/F}$	0.0641	0.0742	0.1041	0.1254	0.1452	0.1816
STD	53.6541	58.8472	61.2351	68.8214	74.3251	81.5372

TABLE 9
RESULTS OF CASE1 MR-T1-T2 IMAGE FUSION ANALYSIS

	DCT [10]	DWT [13]	FFT [11]	IHS [38]	OHWF-GA	Proposed
MI	2.6452	2.9874	2.8741	3.1025	3.6241	3.9356
Entropy	3.4512	3.7841	3.6571	3.9874	4.3214	4.7832
$Q^{AB/F}$	0.0741	0.1240	0.0891	0.1342	0.1542	0.1894
STD	47.8541	56.3201	54.1278	59.8514	76.3214	82.0821

TABLE 10
RESULTS OF CASE2 MR-T1-T2 IMAGE FUSION ANALYSIS

	DCT [10]	DWT [13]	FFT [11]	IHS [38]	OHWF-GA	Proposed
MI	2.4751	2.8915	2.5417	3.1241	3.8457	4.1382
Entropy	3.4152	4.0815	3.6514	4.3451	4.9421	5.3290
$Q^{AB/F}$	0.0778	0.1087	0.1143	0.1341	0.1641	0.2190
STD	56.6214	63.5961	59.6345	68.8741	81.2354	85.4781

C. MR-PET Medical image Fusion

In this section, MR and PET images are fused using our proposed OHWF technique, the examples of fused MR-PET images for dataset 3 and dataset 4 are given in Fig.8. The quantitative results are given in Table 5 and Table 6, in which our proposed technique has higher performance than existing techniques.

D. MR-CT and MR-T1-T2 Medical image Fusion

In this section, MR-CT and MR-T1-T2 fusion are performed using our proposed OHWF technique. The MR soft tissues are mapped to the CT images, where the soft tissues, as well as hard tissues information, can be mapped to a single frame. The quantitative results are reflected in Tables 7 to 10. The attained results demonstrate that the proposed technique has a higher quantitative results compared to existing techniques in terms of mutual information, signal strength and structural similarity. The results of MR-CT fused dataset 1 and dataset 2 images are shown in Fig. 8. The results of MR-T1-MR-T2 fused dataset 1 and dataset 2 images are given in Fig. 8.

The proposed OHWF with HG-GWO produced better quality of fusion than other reported literature fusion works and optimization techniques. The optimum homomorphic domain fusion in our proposed approach mapped more amounts of anatomical as well as metabolic features into a single frame. Our second contribution, hybrid genetic grey wolf algorithm provided dynamic range of scale values.

V. CONCLUSION AND FUTURE DIRECTIONS

In this paper, we proposed Optimum Homomorphic Wavelet Fusion (OHWF) for multi modal medical image fusion is proposed. Here the advantages of wavelet transform and homomorphic filter are mapped into a single image frame. The proposed technique enhances the quality of fusion by combining anatomical and functional features using multi level decomposition. Here we performed MR-PET, MR-SPECT, MR T1-T2 and MR-CT modal fusion for large number of data base images is performed .The optimum scale values are selected using Hybrid Genetic –Grey Wolf Optimization (HG-GWO).

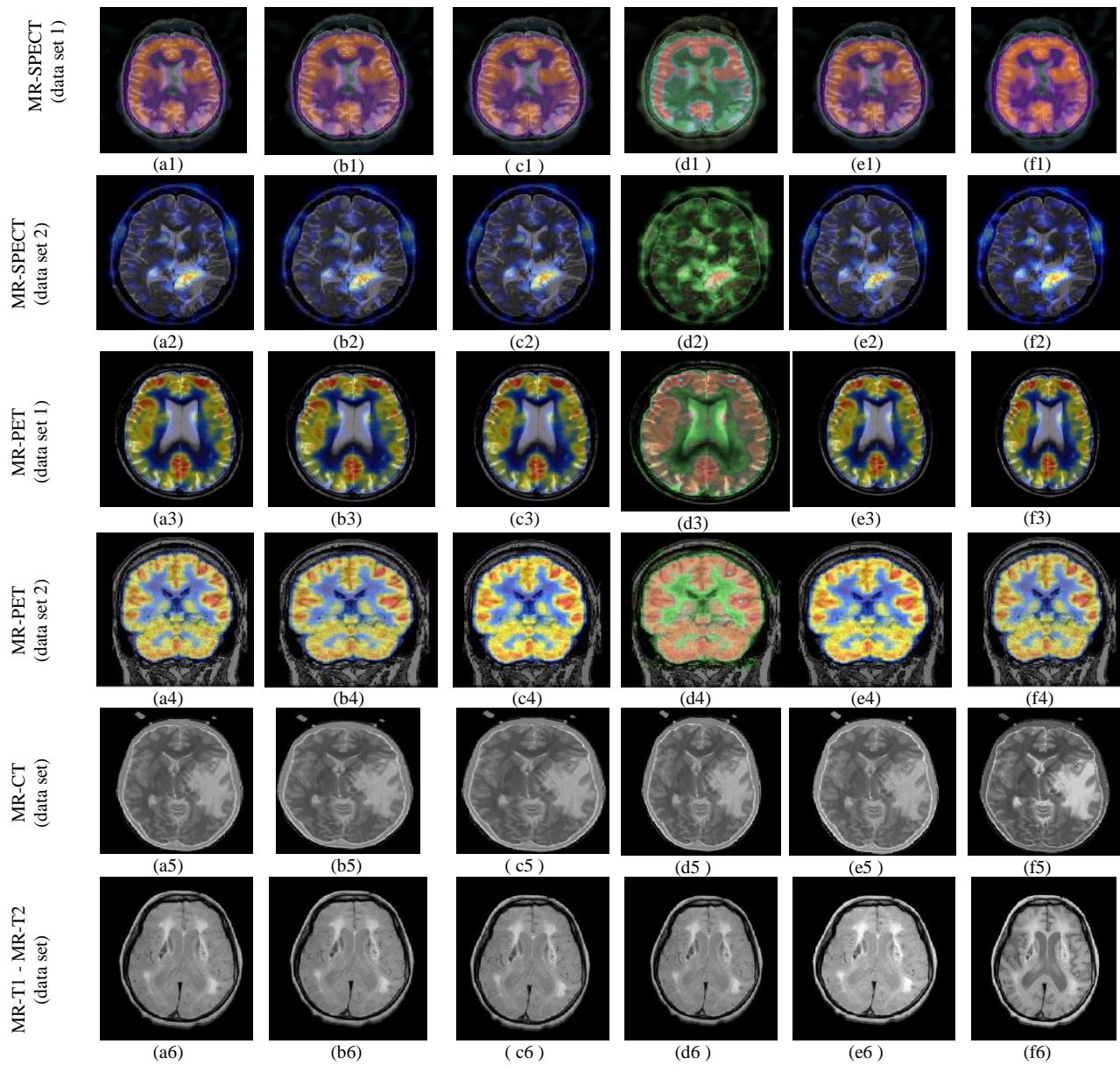


Fig.5. Fused images using (a) DCT (b) DWT [13] (c) FFT (d) IHS (e) OWMF-GA and (f) proposed technique respectively.

TABLE 10
RESULTS OF EXECUTION TIME IN SECONDS

Type of image	GA	PSO	HG-GWO
MR-SPECT	785.2310	421.9830	371.9822
MR-PET	672.8621	392.9830	308.2310
MR-CT	721.4621	402.3218	297.0732
MR-T1-T2	588.1657	338.8221	245.1201

In HG-GWO, the random control parameters are optimally selected using genetic algorithm. For performance analysis OHWF is compared with various fusion techniques in terms of MI, $Q^{AB/F}$ STD and Entropy values. It is found that our proposed approach has greater fusion results than other state of art enhancement techniques. In medical diagnosis, the multilevel decomposition fusion has more importance and is obtained through our technique.

The proposed OHWF technique is used pixel based fusion, in future, feature segmented mapping algorithms

are required to develop for automated perdition of various neurological disorders. In future work, using deep learning algorithms the proposed work can extent for the early stage diagnosis of Alzheimer's diseases and brain tumor.

REFERENCES

1. V. Bhatija, H. Patel, A. Krishn, A. Sahu and A.L Ekuakille, "Multimodal medical image sensor fusion framework using cascade of wavelet and Contourlet transform domains" IEEE Sensors Journal, vol. 15, no. 12, pp. 6783 - 6790, Dec. 2015.
2. R. Srivastava, O. Prakash and A.Khare, "Local energy-based multimodal medical image fusion in Curvelet domain" IET Computer Vision, vol. 10, no. 6, pp. 513 - 527, Sep. 2016.
3. G. Bhatnagar, Q.M. J. Wu and Z. Liu, "Directive contrast based multimodal medical image fusion in NSCT domain" IEEE Transactions on Multimedia, vol. 15, no. 5, pp. 1014- 1024, Aug. 2013.
4. G. Ghimpeanu, T. Batard and M. Bertalmio, A decomposition framework for image denoising algorithms, IEEE Trans. Image Process, vol. 25, no. 1, Jan. 2016 pp. 388-399.
5. X. Liu W. Mei and H. Du "Multi-modality medical image fusion based on image decomposition framework and nonsubsampling shearlet

- transform" *Biomedical Signal Processing and Control*, vol. 40, pp. 1014–1024, Feb. 2018.
6. S. M Darwish "Multi-level fuzzy Contourlet-based image fusion for medical applications" *IET Image Process.*, vol. 7, no.7, pp. 694–700, Oct. 2013.
7. J. Du, W. Li, B. Xiao and Q. Nawaz "Union Laplacian pyramid with multiple features for medical image fusion" *Neurocomputing*, vol.194, pp. 326–339, Jun. 2016.
8. Y. Yang, Y. Que, S. Huang and P. Lin "Multimodal sensor medical image fusion based on type-2 Fuzzy logic in NSCT domain" *IEEE Sensors Journal*, vol. 16, no. 10, pp. 3735–3745, May. 2016.
9. L. Wang, B. Li and L. F Tian "EGGDD: An explicit dependency model for multi-modal medical image fusion in shift-invariant shearlet transform domain" *Information Fusion*, vol. 19, pp. 29–37, Sep. 2014.
10. Y.Lifeng, Z. Donglin, W. Weidong and B. Shanglian "Multi-modality medical image fusion based on wavelet analysis and quality evaluation" *Journal of Systems Engineering and Electronics*, vol. 12, no. 1, pp. 42–48, Mar. 2016.
11. P. Chai, X. Luo and Z. Zhang "Image Fusion Using Quaternion Wavelet Transform and Multiple Features" *IEEE Access*, vol. 5, pp. 6724–6734, Mar. 2017.
12. X. Xu, Y. Wang and S. Chen "Medical image fusion using discrete fractional wavelet transform" *Biomedical Signal Processing and Control*, vol. 27, pp. 103–111, May. 2016.
13. Z. Zhu, Y. Chai, H. Yin, Y. Li and Z. Liu "A novel dictionary learning approach for multimodality medical image fusion" *Neurocomputing*, vol. 214, no. 19, pp. 471–482, Nov. 2016.
14. C. I Chen "Fusion of PET and MR brain images based on IHS and Log-Gabor transforms" *IEEE Sensors Journal*, vol. 17, no. 21, pp. 6995–7010, Nov. 2017.
15. J. Du, W. Li and B. Xiao "Fusion of anatomical and functional images using parallel saliency features" *Information Sciences*, vols. 430–431, pp. 567–576, Mar. 2018.
16. S. S. Chavan, A. Mahajan, S. N Talbar, S. Desai, M. Thakur and A. Dcruz "Nonsubsampled rotated complex wavelet transform (NSRCxWT) for medical image fusion related to clinical aspects in neurocysticercosis" *Computers in Biology and Medicine* vol. 81, no. 1, pp. 64–78, Feb. 2017.
17. C.T Kavitha and C. Chellamuthu "Medical image fusion based on hybrid intelligence" *Applied Soft Computing* vol. 20, pp. 83–94, Jul. 2014.
18. X. Xu, D. Shan, G. Wang and X. Jiang "Multimodal medical image fusion using PCNN optimized by the QPSO algorithm" *Applied Soft Computing* vol. 46, pp. 588–595, Sep. 2016.
19. Y. Liu, X. Chen, H. Peng and Z. Wang "Multi-focus image fusion with a deep Convolutional neural network" *Information Fusion* vol. 36, pp. 191–207, Jul. 2017.
20. G. Bhatnagar, Q.M. J. Wu and Zheng Liu "Human visual system inspired multi-modal medical image fusion framework" *Expert Systems with Applications* vol. 40, no. 5, pp. 1708–1720, Apr. 2013.
21. S. Dasand M. K Kundu, A Neuro-Fuzzy Approach for Medical Image Fusion, *IEEE Transactions on Biomedical Engineering*, vol. 60, no. 12, pp. 3347–3353, Dec 2013.
22. E. Daniel, J. Anitha and J. Gnanaraj "Optimum laplacian wavelet mask based medical image using hybrid cuckoo search – grey wolf optimization algorithm", *Knowledge-Based Systems* vol. 131, no. 1, pp. 58–69, Sep. 2017.
23. E. Daniel, J. Anitha, K.K. Kamaleshwaran and Indu Rani, "Optimum spectrum mask based medical image fusion using Gray Wolf Optimization," *Biomedical Signal Processing and Control*, vol. 34, pp. 36–43, Apr. 2017.
24. A. P. James and B. V. Dasarthy, Medical image fusion: A survey of the state of the art, *Information Fusion* 19 (2014) 4–19.
25. S. Li, X. Kanga, L. Fanga, J. Hub and H. Yin, Pixel-level image fusion: A survey of the state of the art, *Information Fusion* 33 (2017) 100–112.
26. A. Dogra, B. Goyal and S. Agrawal, From multi-scale decomposition to non-multi-scale decomposition methods: a comprehensive survey of image fusion techniques and its applications, *IEEE Access*, vol. 5, pp. 16040–16067, Aug. 2017.
27. R.S. Alves, J.M.R.S. Tavares, Computer image registration techniques applied to nuclear medicine images, *Computational and Experimental Biomedical Sciences: Methods and Applications*, Lecture Notes in Computational Vision and Biomechanics 21 (2015) 173–191.
28. F.P. Oliveira, J.M.R. Tavares, Medical image registration: a review, *Comput. Methods Biomech. Biomed. Eng.* 17 (2014) 73–93.
29. J. M. R. S. Tavares, Analysis of biomedical images based on automated methods of image registration, in: *Advances in Visual Computing*, Lecture Notes in Computer Science, Vol. 8887, Springer, 2014, pp. 21–30.
30. P.M.O. Francisco, T.C. Pataky, J.M.R.S. Tavares, Registration of pedobarographic image data in the frequency domain, *Comput. Methods Biomech. Biomed. Eng.* 13 (6) (2010) 731–740.
31. E.Daniel, J. Anitha, Optimum green plane masking for the contrast enhancement of retinal images using enhanced genetic algorithm, *Optik* 126 (2015) 1726–1730.
32. E.Daniel, J. Anitha, Optimum wavelet based masking for the contrast enhancement of medical images using enhanced cuckoo search algorithm, *Computers in Biology and Medicine* 71 (2016) 149–155.
33. Y.Liu, S. Liu, Z. Wang, A general framework for image fusion based on multi-scale transform and sparse representation, *Information Fusion* 24 (2015) 147–164.
34. Y. Zhuang, K. Gao, X. Miu, L. Han, X. Gong, Infrared and visual image registration based on mutual information with a combined particle swarm optimization – Powell search algorithm, *Optik* 127 (2016) 188–191.
35. J. Li, Z. Peng, Multi-source image fusion algorithm based on cellular neural networks with genetic algorithm, *Optik* 126 (2015) 5230–5236.
36. L. Cao, L. Jin, H. Tao, G. Li, Z. Zhuang, Y. Zhang, Multi-focus image fusion based on spatial frequency in discrete cosine transform domain, *IEEE Signal Processing Letters*, 22 (2015) 220–224.
37. R. Vijayarajan, S. Muttan, Discrete wavelet transform based principal component averaging fusion for medical images, *Int. J. Electron. Commun. (AEÜ)* 69 (2015) 896–902.
38. J.B. Sharma, K.K. Sharma, V. Sahula, Hybrid image fusion scheme using self-fractional Fourier functions and multivariate empirical mode decomposition, *Signal Processing* 100 (2014) 146–159.
39. C. He, Q. Liu, H. Li, H. Wang, Multimodal medical image fusion based on IHS and PCA, *Procedia Eng.* 7 (2010) 280–285.



Ebenezer Daniel Author was born in Kerala, India, in 1989. He received B.Tech degree in electronics and communication engineering from Mahatma Gandhi University, Kerala, India in 2011 and the M.Tech and Ph.D degree in electronics and communication engineering from Karunya Institute of Science and Technology, Coimbatore, India in 2014 and 2017, with respectively.

Currently he is working as an Assistant Professor in Department of Electronics & Communication Engineering, Vignan's Foundation for Science, Technology & Research, in Andhra Pradesh, India. His research areas include Image processing, medical image analysis and bio inspired optimization techniques.